Geometric Accuracy Testing of Orbital Radar Imagery

Abdalla Elsadig Ali
Department of Surveying Engineering, Faculty of Engineering & Architecture, University of Khartoum, P. O. Box 321, Khartoum, Sudan

ABSTRACT: Two spaceborne synthetic aperture side-looking radar SAR images covering two different areas were tested for geometric accuracy in order to assess the suitability of the present spaceborne radar systems for topographic mapping applications. One image was optically processed using the ERIM tilted-plane optical processor, and the other was digitally processed using the Royal Aircraft Establishment (RAE) Experimental SAR Processing Facility (ESPF). The two test images were transformed to the terrain coordinate system using different mathematical algorithms. The root-mean-square errors of the discrepancies between the known terrain coordinates and the transformed image coordinates of the points were then computed and compared with NATO specifications for topographic mapping. The results show that the geometric fidelity of the present spaceborne SAR systems is compatible with planimetric mapping requirements at 1:150,000 scale and smaller depending on the method of processing the SAR data (i.e., digital or optical), the nature and topography of the area being mapped, the number and distribution of ground control points used, and the mathematical algorithm employed in transforming the SAR image. For other earth science applications where the required geometric accuracy is not very stringent, spaceborne side-looking radar (SLR) imageries will have much to offer.

INTRODUCTION

FOR A VERY LONG TIME, the development of an all-weather, day-and-night mapping system has been desired by the topographic community. Side-looking radar is one system that possesses such a capability. In many parts of the globe, there were indeed successful mapping projects using side-looking radar. Project RAMP in Panama, PRORADAM and RADAM in South America, and NIRAD in Nigeria are examples of these successful projects. In most of these projects, controlled, semi-controlled, or simple uncontrolled mosaics were constructed and used as base-maps (mostly at 1:250,000 scale) for geological, land-use, or vegetational purposes. The success of these radar projects made the National Aeronautic and Space Administration (NASA) decide to mount a side-looking radar system on-board the then-new Seasat Satellite.

The present contribution reports on the metric accuracy of Seasat Satellite radar system for very small-scale planimetric mapping (1:100,000 and smaller). Indeed, many countries in the third world have very poor topographic coverage, in particular, those around the equatorial belt due to lack of aerial photographic coverage (due to clouds). An insight into the way of practical testing of spaceborne side-looking radar to determine the accuracies attainable will reveal the extent to which such countries hope to perform topographic mapping using side-looking radar.

TEST MATERIAL

Two images of Seasat SLR were available for the experiment.

One image covers the banks of the River Tay in Scotland for a distance of about 40 km of its length. The terrain in this test area is quite varied in topography, and topography relief ranges from sea level to around 350 metres. The image had been *optically processed* using a tilted-plane optical processor owned by the Environmental Research Institute of Michigan (ERIM), and was at a 1:250,000 scale and had a nominal resolution of about 60 m (see, e.g., Kozma *et al.* (1972) for the construction and operation of this system).

The second image covers parts of East Anglia in England and had been *digitally processed* using the Experimental SAR Processing Facility of the Rayal Aircraft Establishment (RAE) at Farnborough in England. The software for this system has been written in collaboration with System Designers Ltd. (SDL), Frimley, Survey (England). Figure 1 is a block diagram of this digital processing facility. Up to four independent looks are available form this processing system, each look being processed separately. Within the limits of the radar system, the azimuth resolution may be selected at will. Also, the image may be arbitrarily aligned with the satellite line of sight. Adjacent images may be exactly registered with one another.

The first step in processing the SAR data takes place at the satellite data receiving station where the SAR data record is recorded on high density digital tapes (HDDTs). These are then processed frame by frame (50 km by 50 km) and transferred to a 300 Mbyte disk using a Prime 300 Computer. When this process is complete, data are again transferred onto 1600 BPI computer Compatible Tables (CCTs). This serves as input to a Prime 400 equipped with an array processor which does the function of range compression by Fourier Transform. The process of co herent summation (azimuth compression) is then carried out together with the necessary radiometric and geometric corrections. The image pixels are then sorted and a final image tape is produced in a line-by-line format for direct use if necessary.

This procedure allows correction for many geometric errors. However, range curvature errors are corrected to first order only; hence, one should anticipate the existence of some residual errors resulting from this source and variations of topography because no stereo-radar coverage was obtained from Seasat.

The area is fairly flat with topography ranging from sea level to around 90 metres. This image was at a scale of 1:150,000 and had a resolution of 25 m.

PREPARATION AND MEASUREMENT

This stage began with selection and marking of prominent points on the optically processed River Tay image and the digitally processed East Anglia image. Many difficulties, however, were experienced in the selection of control points to be used for the geometric testing experiment. These arise from the lack of certainty as to the exact positions of those features shown on the SLR images which were well defined on the map. On many occasions, one had to be satisfied with points such as centers of islands in lakes, river junctions, sharp bends along drainage systems, etc. This applied to both images, although to a lesser extent in the digitally processed image. As a result, irregular distribution patterns of ground control were obtained.

PHOTOGRAMMETRIC ENGINEERING AND REMOTE SENSING,
Vol. 53, No. 11, November 1987, pp. 1533–1537.

0099-1112/87/5311–1533$02.25/0

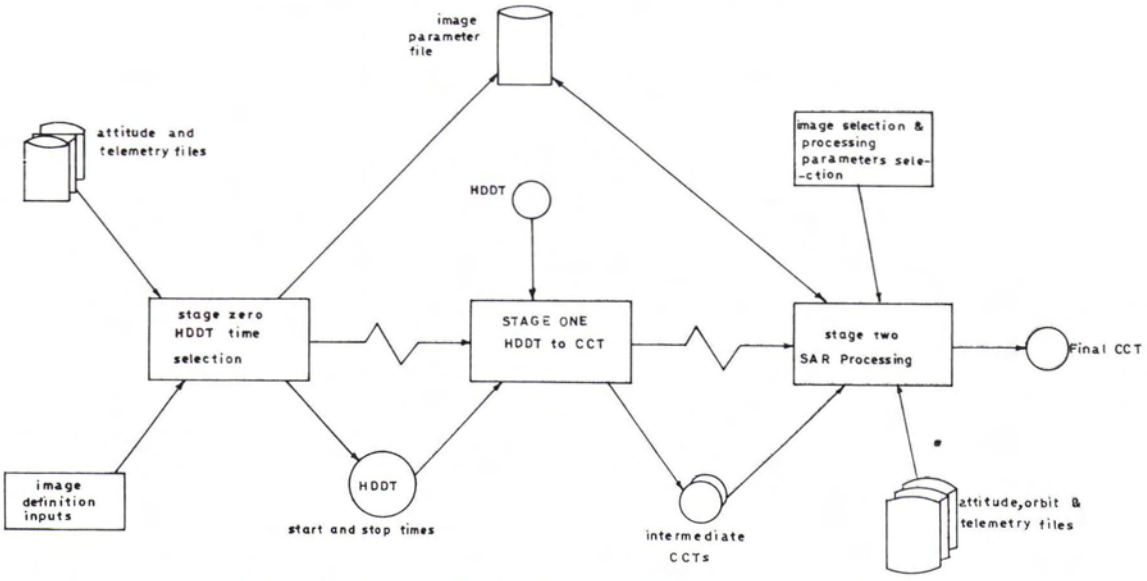

FIG. 1. RAE/SDL Experimental SAR Processing Facility (ESPF) block diagram.

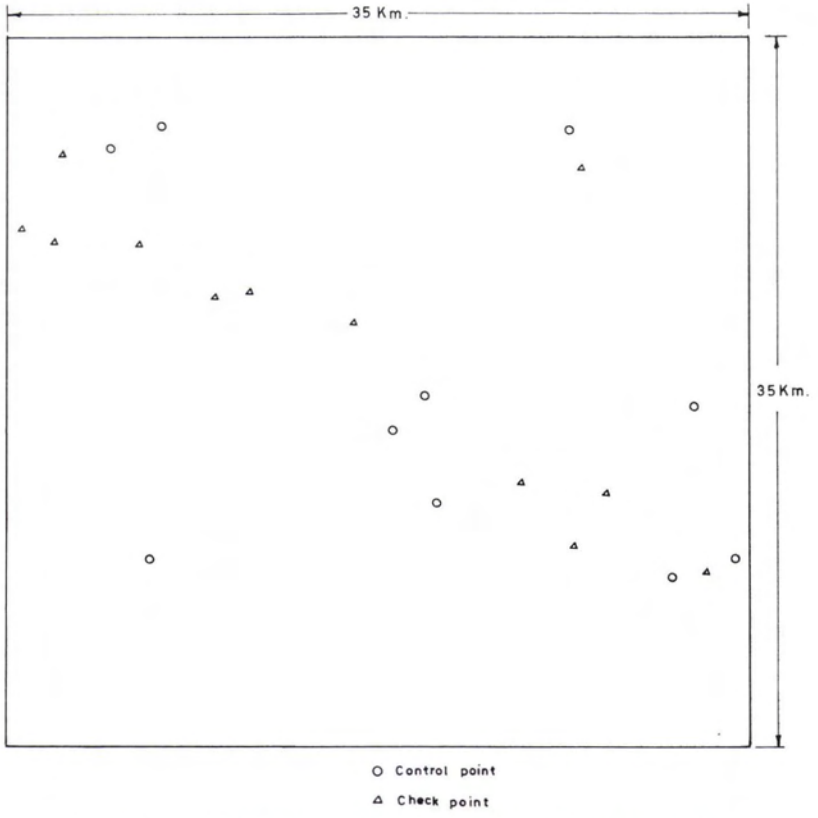

FIG. 2. Control distribution pattern on the optically processed image.

A total of 22 points were selected on the River Tay test image and 99 points on the digitally processed image of East Anglia. The distribution patterns of these points are shown in Figures 2 and 3, respectively. Some of the points were used as control points on which the transformation of the imagery to fit the ground was based, while the rest of the points were used as check points for the purpose of assessing the metric accuracy of the images.

The image coordinates of the points were measured using a Houston Hi-Pad digitizer with a 100-μm resolution. This resolution seems appropriate, taking into account the rather poor resolution of the two test images.

The ground coordinates of the points were derived from 1:50,000-scale maps of the test areas by means of a coordinatograph with an accuracy of ±0.1 mm.

COORDINATE TRANSFORMATION

The procedure for testing the metric accuracy of the images had been to transform the images using three different mathematical algorithms. These are

- Linear conformal transformation
- Affine transformation, and
- Polynomial transformation.

The latter consists of the following equations which had been specially designed to cater for the various residual errors left in

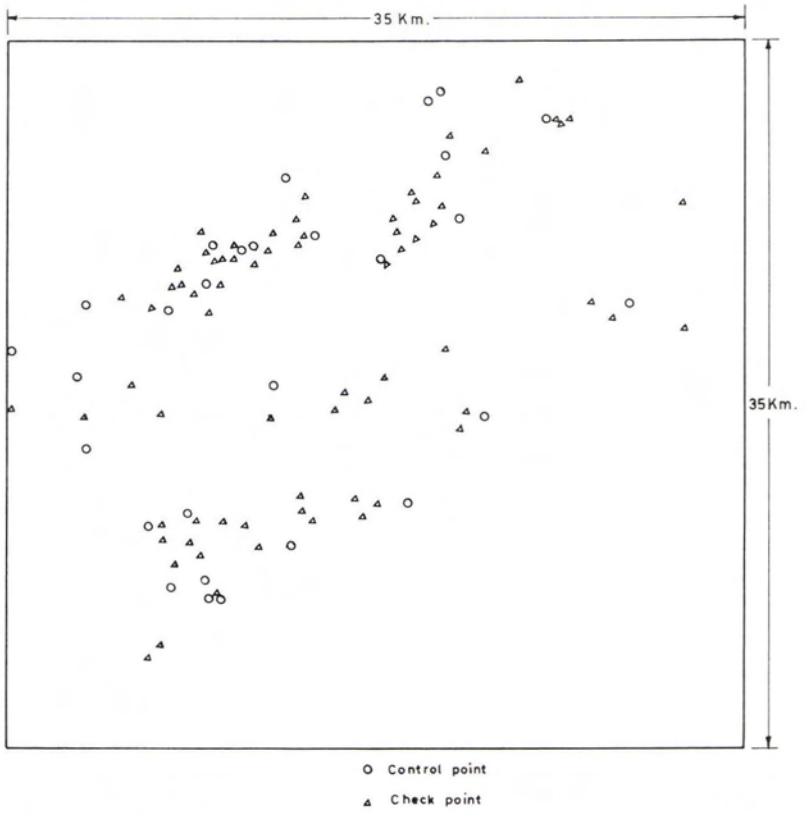

FIG. 3. Control distribution pattern on the East Anglia test area image.

the processed SLR images after the processing stage (Ali, 1982):

$$X = n_o + n_1x + n_2y + n_3xy + n_4x^2 + n_5x^2y + n_6x^3 + n_7x^3y;$$
$$Y = m_o + m_1x + m_2y + m_3xy + m_4x^2 + m_5x^2y + m_6x^3 + m_7x^3y$$

where x, y are image coordinates; X, Y are the corresponding ground coordinates; and n_i, m_i are the unknown transformation parameters.

TEST RESULTS

Tables 1 and 2 summarize the results obtained from the tests of the optically processed River Tay image and the digitally processed Eat Anglia image. For the polynomial transformation, the root-mean-square error (RMSE) of the discrepancies at the measured points was first computed using the full terms of the polynomial. These are then dropped one by one and the RMSE recomputed. The root-mean-square errors, σ, are calculated using the formulae

$$\sigma_1 = \left[\frac{\Sigma v^2}{n-u}\right]^{1/2} \text{ for the control points; and}$$

$$\sigma_2 = \left[\frac{\Sigma v^2}{n}\right]^{1/2} \text{ for the check points}$$

where

v = residual error at a control or check point;
n = number of points used, and
u = minimum number of control points required to solve the system of equations

COMPARISON OF RESULTS FROM THE TWO IMAGES

Close inspection of Tables 1 and 2 reveals the fact that, while the optically processed image fits quite poorly to the ground after a linear conformal transformation, with the digitally

TABLE 1. RESULTS OF THE OPTICALLY-PROCESSED IMAGE OF TAY AREA

Imagery	No. of terms in Polynomial	Control Points (n = 9)			Check Points (n = 12)		
		σ_X(m)	σ_Y(m)	σ_P(m)	σ_X(m)	σ_Y(m)	σ_P(m)
Optically Processed	8	26	90	94	79	74	108
	7	59	105	120	173	110	205
	6	51	103	115	172	156	232
	5	81	147	168	67	86	109
	4	79	126	149	63	84	105
	3	69	124	142	63	86	107
	Linear Conformal Transformation	134	517	534	240	247	344
		(n = 2)		148	474	497	

TABLE 2. RESULTS OF THE DIGITALLY PROCESSED EAST ANGLIAN TEST AREA

Imagery	No. of terms in Polynomial	Control Points (n = 28)			Check Points (n = 71)		
		σ_X(m)	σ_Y(m)	σ_P(m)	σ_X(m)	σ_Y(m)	σ_P(m)
Digitally Processed	8	23	26	35	26	26	37
	7	24	25	35	25	26	36
	6	25	28	38	28	29	40
	5	27	29	40	27	27	38
	4	26	36	44	28	32	43
	3	25	35	43	28	31	42
	Linear Conformal Transformation	26	38	46 (n = 2)	26	39	47
		–	–		36	38	52

processed image this transformation produces results which are not too different from those obtained from the higher order polynomial. This suggests that, for topographic mapping applications from side-looking radar, digital processing techniques should be employed because these have the capability of increased flexibility in handling geometric corrections and in producing better interpretable images.

Having said that, one must ask why some geometric deformations still exist in the transformed SAR image even after employing the excellent method of digital image processing. However, an immediate answer can be that, because Seasat SAR acquired data in monoscopic form only, the presence of radar relief displacement errors, however small they may be, must be understood. If this is combined with the residual errors left after processing due to range curvature (Guignard, 1980), planimetric errors of up to one resolution element can be expected in the final digitally processed image.

Radar relief displacement errors can be minimized by incorporating a radar interferometer (Graham, 1974) which would make it possible to measure heights of objects which can be used later in the digital processing stage to correct for relief displacement errors. Unfortunately, this system was not onboard the Seasat satellite.

On the other hand, relief displacement errors could also be minimized by employing the technique of digital monoplotting from single radar images. A digital terrain model (DTM) of the imaged area can be constructed from existing topographic maps of the area. This can be used to calculate heights of transformed features on the image which will allow computation of relief displacement errors of individual points. This again was not employed during the digital processing of the SAR imageries.

As regards errors caused by residual range curvature, the functional model of this error could be extended to include the non-linear terms, thus reducing its effect substantially.

COMPARISON WITH OTHER SEASAT GEOMETRIC TESTS

It is interesting to compare the results of this experiment with other tests carried out for testing the metric accuracy of Seaset SAR imagery. Mohammed (1981) achieved similar results over the same area of East Anglia. He used a general polynomial of the form

$$X = a_0 + a_1x + a_2y + a_3x^2 + a_4y^2 + a_5xy + a_6y^3 + a_7x^2y + a_8xy^2 + a_9x^2y^2 + a_{10}x^3 \text{ and}$$

$$Y = b_0 + b_1x + \ldots + b_{10}x^3.$$

The difference between the tests carried out in this experiment and Mohammed's tests lies in the fact that Mohammed measured

TABLE 3. MOHAMMED'S RESULTS OF THE EAST ANGLIAN IMAGE (IN METRES)

No. of control Points	1st sub-swath								2nd sub-swath							
	n = 4		n = 7		n = 10		n = 30		n = 4		n = 7		n = 10		n = 24	
No. of check Points	n = 26		n = 23		n = 20		n = 0		n = 20		n = 17		n = 14		n = 24	
	σ_X	σ_Y	σ_X	σ_Y	σ_X	σ_Y	σ_X	σ_Y	σ_X	σ_Y	σ_X	σ_Y	σ_X	σ_Y	σ_X	σ_Y
Linear	297	9544	362	934	363	900	214	947	137	360	131	372	136	339	127	313
Affine	55	110	53	120	52	115	50	112	84	135	73	120	71	115	71	103
6-term poly	–	–	41	69	34	76	37	46	–	–	34	61	42	44	32	51
7-term poly	–	–	37	48	38	47	36	40	–	–	36	44	32	37	37	33
'Specific' Polynomials	–	–	47	52	45	50	39	47	–	–	41	57	42	51	38	49

No. of control Points	3rd Sub-Swath								2nd Sub-Swath							
	n = 4		n = 7		n = 10		n = 32		n = 4		n = 7		n = 10		n = 13	
No. of check Points	n = 28		n = 25		n = 22		n = 0		n = 9		n = 6		n = 3		n = 0	
	σ_X	σ_Y	σ_X	σ_Y	σ_X	σ_Y	σ_X	σ_Y	σ_X	σ_Y	σ_X	σ_Y	σ_X	σ_Y	σ_X	σ_Y
Linear	237	389	272	381	292	407	222	396	143	413	136	147	310	308	165	403
Affine	56	79	67	92	64 93	57	80	47	56	43	55	43	57	43	57	
6-term poly	–	–	46	55	44	53	34	45	–	–	42	67	45	45	46	46
7-term poly	–	–	37	49	36	48	34	41	–	–	33	55	32	44	25	48
'Specific' Polynomials	–	–	35	44	41	41	35	44	–	–	37	52	25	52	25	51

and transformed images from each of the four subswaths of the Seasat SAR coverage. Table 3 shows the results obtained by Mohammed. It is noticeable from this table that the results of Mohammed's tests using higher degree polynomials were of the same order as those reported in this paper though considerably larger in magnitude. It is also noticeable that the original image of East Anglia supplied to Mohammed contained large affine scale errors as shown by the abrupt drop in the RMSE values when an affine transformation was applied. Also, the use of the higher order polynomials had a much more substantial effect than was apparent in the image measured in this experiment.

ASSESSMENT OF SEASAT GEOMETRIC ACCURACY FOR PLANIMETRIC MAPPING

A convenient set of standards to use in assessing metric accuracy of any imaging sensor are the NATO specifications for topographic mapping. For maps at 1:600,000 scale and larger, the planimetric accuracy of well-defined features for class A maps is given as $\sigma_p = \pm 0.3$ mm at map scale. Figure 4 shows the relation, using this criteria, between map scale and required planimetric accuracy. Using the accuracy figures obtained after testing the two Seasat images of this experiment, it should be noted that the geometrical accuracy of the digitally processed SAR/image is compatible with mapping at the scale of 1:150,000. For the optically processed image of the River Tay test area, the accuracy attainable with the Seasat SAR imagery is markedly lower; hence, planimetric mapping at scales 1:350,000 and smaller can be contemplated. Thus, in purely geometric terms, the Seasat SAR imagery has definitely some possibilities for small-scale planimetric mapping. For other Earth science applications where the required geometric accuracy is rather modest, spaceborne SLR will definitely have much to offer.

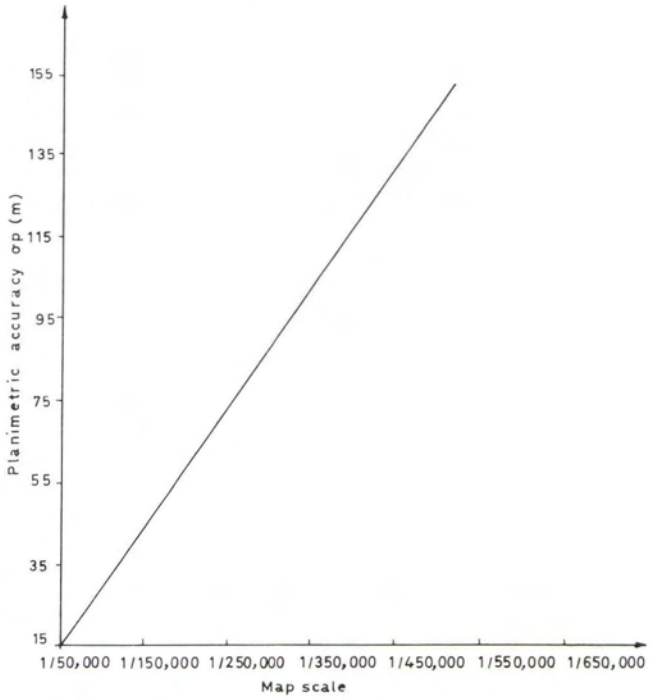

FIG. 4. Planimetric detail accuracy at different scales.

CONCLUSION

The experiment has confirmed the fact that the geometric accuracy of SLR imagery falls far below that of conventional photographic images, the attainable accuracy being dependent on many factors, the most important of which are the method of processing the SAR data and the nature and topography of the area being mapped.

The experiment has also shown that it is possible to extract metric information from spaceborne radars at an accuracy standard sufficient for the purposes of many developing countries, particularly those with continuous cloud cover which makes acquisition of photographic images impossible. The geometric errors present on the transformed SLR images would have been much less if digital monoplotting techniques had been employed during the processing stage or if the functional model for range curvature had been extended to include higher order terms.

REFERENCES

Ali, A.E., 1982. *Investigation of Seasat-A Synthetic Aperture Radar for Topographic Mapping*. Ph.D. Thesis, University of Glasgow, 460 p.

Grahma, L.C., 1974. *Synthetic Aperture Radar Applications to Earth Resources Development*. Goodyear Aerospace Corporation Report, NO. GERA-2010.

Guignard, J.P., 1980. The I.S.P. SAR Processing Workshop Group Activities. *Proceedings of I.S.P. International Congress*, Hamburg, F.R.G., Vol. B9, p. 223–246.

Kozma, A., E. N. Leith, and N.G. Massey, 1972. Tilted Plane Optical Processor. *Applied Optics*, Vol. 11, No. 8, p. 1766–1777.

Mohammed, M.A., 1981. *Photogrammetric Analysis and Rectification of Landsat MSS and Seasat SAR Images*. Ph.D. Thesis, University College, London 1980 p.

(Received 15 September 1986; revised and accepted 10 July 1987)

Forthcoming Articles

Michael H. Brill and *James R. Williamson*, Three-Dimensional Reconstruction from Three-Point Perspective Imagery.

T. L. Coleman and *O. L. Montgomery*, Soil Moisture, Organic Matter, and Iron Content Effect on the Spectral Characteristics of Selected Vertisols and Alfisols in Alabama.

Tung Fung and *Ellsworth LeDrew*, Application of Principal Components Analysis for Change Detection.

Kurt Kubik and *Dean Merchant*, Photogrammetric Work Without Blunders.

Robert D. Lamb, H. E. McGarrah, and *J. D. Eick*, Close-Range Photogrammetry with Computer Interface in Dental Research.

Donald G. Leckie, Factors Affecting Defoliation Assessment Using Airborne Multispectral Scanner Data.

Fang Lei and *H. J. Tiziani*, A Comparison of Methods to Measure the Modulation Transfer Function from the Image Structures of Aerial Survey Lens Systems.

Ted D. Needham and *James L. Smith*, Stem Count Accuracy and Species Determination in Loblolly Pine Plantations Using 35-mm Aerial Photography.